Published in final edited form as:

Nat Neurosci. 2009 January ; 12(1): 35–43. doi:10.1038/nn.2236.

Transient neurites of retinal horizontal cells exhibit columnar tiling via homotypic interactions

Rachel M. Huckfeldt[1], **Timm Schubert**[1,#], **Joshua L. Morgan**[1,#], **Leanne Godinho**[2], **Graziella Di Cristo**[3], **Josh Z. Huang**[3], and **Rachel O.L. Wong**[1]

[1]Dept. of Biological Structure, University of Washington, 1959 NE Pacific St., WA 98195, USA

[2]Institute of Stem Cell Research, Helmholtz Zentrum München, Ingolstädter Landstrasse 1, D-85764 Neuherberg, Germany

[3]Cold Spring Harbor Laboratory, 1 Bungtown Road, Cold Spring Harbor, NY 11724, USA

Abstract

Sensory neurons with common function are often non-randomly arranged and form dendritic territories that exhibit little overlap or tiling. Repulsive homotypic interactions underlie such patterns in cell organization in invertebrate neurons. In mammalian retinal horizontal cells, however, it is unclear how dendro-dendritic repulsive interactions can produce a non-random distribution of cells and their spatial territories because mature horizontal cell dendrites overlap substantially. By imaging developing mouse horizontal cells, we found that upon reaching their final laminar positions, these cells transiently elaborate vertical neurites that form non-overlapping columnar territories. Targeted cell ablation revealed that the vertical neurites engage in homotypic interactions resulting in tiling of neighboring cells prior to establishment of their dendritic fields. This developmental tiling of transient neurites correlates with the emergence of a non-random distribution of the cells, and could represent a mechanism that organizes neighbor relationships and territories of neurons of the same type before circuit assembly.

Throughout the nervous system, neurons within the same functional class are often organized in stereotypic spatial patterns. In many sensory circuits, complete and non-redundant representations of sensory information are attained by a tiling arrangement such that the dendritic arbors of the same cell type show little or no overlap. Previous studies in invertebrates such as the leech1 and *Drosophila*2,3 suggest that dendritic tiling is regulated by homotypic repulsive interactions between the dendrites of neighboring cells. However, in some vertebrate systems, dendritic arbors overlap extensively even though the cells are non-randomly distributed4,5. It is not readily apparent, therefore, how homotypic interactions can allow for the extensive overlap between the dendritic territories of sensory neurons yet enable the cells to attain a non-random, mosaic-like arrangement. One possibility is that

[#]These authors contributed equally

Author contributions

R.M.H. and R.O.L.W conceived the study and wrote the manuscript; R.O.L.W. supervised the project. R.M.H., T.S., J.L.M. and L.G. carried out the experiments and/or data analysis. J.L.M. wrote the MatLab routines for the analysis. G.D.C. and J.Z.H. provided the G42 mice. All authors contributed to preparation of the manuscript and agree to all its content, including data as presented.

homotypic repulsive interactions initially act to organize cells into a non-random distribution with territories that tile as in invertebrates. Once the cells have attained approximate positions, repulsive interactions could be down-regulated, allowing dendrites of a cell to extend well into neighboring territories. Here, we investigated this possibility by focusing on horizontal cells of the mammalian retina, which form a regular mosaic but exhibit substantial overlap of their dendritic territories at maturity.

By postnatal day 10 (P10) in the mouse retina, any point in space is covered by the lateral dendritic arbors of six to seven neighboring horizontal cells6. Interestingly, horizontal cells are non-randomly distributed at birth, even before the development of dendritic arbors. Thus, it is unclear how dendro-dendritic interactions can account for the regularity in the distribution of these neurons. However, embryonic and neonatal horizontal cells possess vertically-oriented neurites forming columnar arbors that completely disappear as laminar dendritic arbors become confined to a specific retinal depth with maturation7,8. Because these vertical columnar arbors are formed during the earliest period when horizontal cells demonstrate a non-random distribution6 it is conceivable that homotypic interactions between horizontal cells, which have been postulated to regulate their spatial distribution9,10, are mediated by the transient neurites.

To test this hypothesis, we performed multi-photon time-lapse imaging of acutely isolated embryonic and early postnatal retinas from the G42 transgenic mouse line11 in which horizontal cells express green fluorescent protein (GFP) under the control of the *GAD67* promoter. We visualized the behavior of the transient vertical processes during horizontal cell migration in the embryonic retina and throughout early neonatal development. We discovered that prior to the development of laminar dendritic arbors, the vertical neurites of neonatal horizontal cells form territories with surprisingly little overlap. Targeted laser ablation of early neonatal horizontal cells unmasked constraints on the size and shape of the vertical neuritic arbor of horizontal cells; cells bordering the ablated region extended their neurites towards the ablation zone within several hours post-ablation. This rapid response was not observed at later neonatal ages after horizontal cells had elaborated lateral and overlapping dendritic arbors. We suggest that repulsive homotypic interactions between developmentally transient processes, rather than dendro-dendritic interactions, establish the initial territories and neighbor relationships of horizontal cells and can conceivably contribute to spatial arrangements in mature circuits.

RESULTS

Horizontal cells express GFP in G42 retina

GFP expression in the G42 retina was observed in two spatially distinct populations of neurons in the inner nuclear layer (INL). GFP-positive cells at the outer boundary of the INL exhibited a spatial organization consistent with that of horizontal cells. Intracellular dye-filling of this population at P5 and P18 to visualize the morphology of individual GFP-positive cells confirmed their cell-type identity (Fig. 1a). At both ages, the dendritic arbors of the injected cells radiated outward from their somata and extended to or beyond the cell bodies of their immediate neighbors. These characteristics and the presence of an axon

suggest that the GFP-positive cells in the outer retina were indeed the single morphological class of horizontal cell found in the mouse retina12.

GFP expression by horizontal cells was not uniform across the retina. At P3, expression was high in dorsal retina and markedly lower in ventral retina (Supplementary Fig. 1 online). This difference persisted until at least P10. We performed immunostaining for calbindin, a marker of horizontal cells13, to determine what proportion of the horizontal cell population expressed GFP in the dorsal retina. In high-density regions at P3 and P9, we found that over 90% of calbindin labeled cells expressed GFP within the image field (Fig. 1b). For subsequent experiments, imaging was performed within these high-density fields.

Horizontal cells transiently exhibit radial morphology

During embryonic and early postnatal development, horizontal cells attain their final depth in the outer retina and their neuritic arbors undergo a transformation from a radial to a laminar organization7,8,14. GFP expression by horizontal cells in the G42 line allowed these morphological changes to be visualized with a degree of detail not readily achieved by immunolabeling methods (Fig. 2). At embryonic day 17.5 (E17.5), horizontal cell somata occupied varied retinal depths between the amacrine cells and their eventual position at the outer retina. Horizontal cells could be distinguished from amacrine cells by their larger and typically brighter somata. Embryonic horizontal cells possessed basal processes oriented toward the inner retina as well as apical processes extending towards the outer limiting membrane (OLM).

At birth, a clear spatial separation was evident between the positions of GFP-expressing horizontal cells and amacrine cells. The apical processes of horizontal cells were more profuse and elaborate, and some contacted the OLM. At P3, cell bodies occupied a near-uniform retinal depth, and many cells lacked basal processes. The apical vertical processes were less numerous, and a complex lattice of laterally-directed processes occupied a broad band above the cell bodies. A rudimentary laminated plexus appeared by P5, although occasional vertical processes were still observed. By P9, a narrowly confined lamina was present that resembled the organization seen at structural maturity (P21). Together, these observations emphasize the significant structural reorganization horizontal cells undergo during development and corroborate previous observations from immunostaining methods15,8 and electron microscopy7.

Horizontal cells exhibit lateral somal movements

After becoming post-mitotic at the apical surface of the retina, horizontal cells migrate to the vitreal surface of the inner retina before returning to the outer retina16. The varied depths of horizontal cell somata in the embryonic retina observed here thus reflect different stages in their migration to the outer retina (Fig. 2). To provide the first direct evidence for the radial migratory behavior of horizontal cells in the mouse retina, we conducted time-lapse multiphoton imaging of GFP-expressing horizontal cells in embryonic G42 retina. We frequently observed horizontal cells migrating toward the apical surface (Fig. 3a). Of 17 cells (n = 3 retinas) that migrated radially, 12 migrated apically and 5 migrated basally. The migrating neurons possessed one or two sparsely branched apical processes (Fig. 3a–d) that

exhibited retraction and extension (Fig. 3a). This simple morphology contrasts with the more numerous and highly branched vertically-oriented neurites of horizontal cells that have reached more apical depths (Fig. 3a, black asterisk).

In addition to radial migration, we also observed lateral somal translocation of embryonic horizontal cells (n = 3 retinas; 16 cells; Fig. 3b). Cell somata squeezed through thick, laterally directed neurites (Fig. 3b and Supplementary Video 1 online). In these isolated retinas, lateral somal translocation was slow: As many as six hours separated the appearance of a dilated neurite adjacent to the soma and the translocation of the cell body. Lateral somal translocation was most frequently observed in somata at a depth similar to that of the eventual horizontal cell layer. Our time-lapse data thus provide the first real-time view of a short distance cell-positioning mechanism previously inferred from X-inactivation studies17,18.

We next examined whether migrating horizontal cells exhibit specific intercellular spatial relationships by calculating the density recovery profile (DRP)19 for the centers of horizontal cell somata at E17–18 (n = 3 retinas, n = 388 cells; Fig. 3e). A dip in the DRP below the average somal density suggests the presence of an exclusion zone around the cell body in which the probability of encountering another horizontal cell is reduced. Such a zone was absent around the somata of embryonic horizontal cells. The effective radius of the DRP (R_e = 6.7 μm) was roughly equal to a cell body diameter (average somal radius for E17–18 horizontal cells = 3.67 ± 0.07 μm, n = 24 cells). The equivalent radius of the two-dimensional (x-y) territories of these immature horizontal cells (R_t = 10.7 μm) exceeded the effective radius of the DRP, meaning that in the x-y dimension, cell bodies of neighbors were found within the lateral extent of a cell's territory. This was apparent in some migrating cells that appeared stacked on top of each other when they were viewed in the x-y dimension (Fig. 3c,d; orange and red cells). The lack of an exclusion zone is also evident when viewing the spatial auto-correlogram of the cells at E17–18 (Fig. 3e). Thus, it appears that E17–18 horizontal cells have yet to form distinct territories with specific neighbor relationships, most likely because they possess few neurites at these ages.

Radial arbors of neonatal horizontal cells tile

By birth, the majority of horizontal cell bodies forms a single lamina in the outer retina (Fig. 2). We thus performed time-lapse multiphoton imaging of P0–3 retinas from the G42 transgenic line to: (i) examine the behavior of the vertical neurites on a single cell basis, and (ii) determine how the morphological changes of a single cell’s neurites relate spatially to those of its neighbors once this layer has formed. We found that the vertical neurites of neonatal horizontal cells were highly dynamic. Extension and retraction of individual processes could be followed across short intervals (1–2 hrs) (Supplementary Fig. 2 online). Over longer periods (6 to 7 hours), reorganizations of the vertical processes were so extensive that it was often impossible to track individual neurites (data not shown). The extension and retraction of OLM-directed vertical neurites continued even after a rudimentary neuritic lamina had formed at P3 (Supplementary Fig. 2b online). These vertical neurites also differed from axon-like processes that appeared and grew rapidly at this age (Supplementary Fig. 3 online).

When viewed *en face*, the vertical neurites of P0–3 horizontal cells formed distinct, columnar territories. To better visualize these territories, individual cells were segmented and colorized in three-dimension (see Methods) and assigned two-dimensional territories with a custom dilation-erosion software program (Fig. 4a–c). Territory area and overlap, defined as the percentage of a cell's territory shared with a neighboring cell, were assessed over time. Changes in the size of an individual cell's territory could be appreciated over 6 to 8 hour intervals (Fig. 4c), although at a population level, the initial mean area of 1101 ± 71 μm^2(mean ± s.e.m.; n = 3 retinas, 16 cells) remained constant (Fig. 4d; 0 hours vs. 6–7 hours: P = 0.64; 0 vs. 12–5 hours: P = 0.60; Wilcoxon signed rank test). Territory overlap was 4.8 ± 0.7% and remained relatively stable over these intervals (Fig. 4e; 0 hours vs. 6–7 hours: P = 0.83; 0 vs. 12–15 hours: P = 0.59). Importantly, even the small amount of overlap reported here is likely to be an overestimate because our territory assignment did not exclude the axon-like processes of horizontal cells observed to project far into, and sometimes beyond, neighboring territories (Fig. 4a–c). Territory area and overlap were thus relatively constant despite extensive changes in individual cell morphology.

Close physical proximity between the vertical neurites of adjacent cells was frequently observed in z-projections of the segmented and colorized horizontal cells. When cell pairs were reconstructed in three-dimension, we found that apparent appositions were often due to abutting neurites (Supplementary Fig. 4 online). Cell pairs formed on average 0.77 ± 0.09 appositions (range 0–3 at any one time point, n = 79 cell pairs, 3 retinas) with each other. These appositions and the maintenance of minimal territorial overlap are consistent with the notion that homotypic interactions between transient vertical neurites maintain territorial spacing between neighboring horizontal cells prior to the establishment of their lateral dendritic arbors.

We next examined whether the somata of horizontal cells were more regularly distributed when the vertical arbors show tiling. The dip in the DRP clearly indicated the presence of an exclusion zone for early neonatal horizontal cells (P2; n = 265 cells; Fig. 4f). An exclusion zone is also apparent in the auto-correlogram. The effective radius of the DRP (R_e = 15.1 μm) was much greater than the equivalent radius of a cell body (mean radius of the somata at P2 is 3.8 ± 0.04 μm; n = 61 cells) and closely matched the equivalent radius of their territories (R_t = 14.6 μm). Thus, shortly after birth and in the presence of vertical neurites forming tiling columnar arbors, the horizontal cell body mosaic clearly assumed a non-random distribution. Our observations support previous measurements demonstrating that horizontal cell body mosaic is non-random by birth6.

Neighbor interactions restrict vertical arbor territory

To investigate the possibility that neonatal horizontal cells exhibit repulsive homotypic interactions, we performed targeted cell ablation with the infrared laser and monitored the behavior of the remaining neighboring cells. Between 2 and 18 neurons in high density fields of horizontal cells were targeted for sequential ablation at P1 to P3. The impact of the laser and subsequent cell death upon neighboring horizontal cells and the local cellular environment was negligible (Supplementary Fig. 5 online).

Marked space-filling into regions vacated by the ablated horizontal cells was consistently observed (n = 4 retinas, 5 fields; Fig. 5a). This process began as early as 90 minutes post-ablation, and neurite density in the ablated zone continued to increase during the following 12–14 hours of imaging. The size of the zone determined the extent to which space-filling was complete: When two or three cells were ablated, colonizing neurites completely filled the space (Fig. 5a,b, Supplementary Videos 2 and 3 online) whereas when seven to eighteen cells were ablated, space-filling was less complete (Supplementary Video 4 online). In contrast, space-filling was not observed at all following horizontal cell ablation in P7–8 retinas (n = 2 retina, 4 fields) within a similar post-ablation period (Supplementary Fig. 6 online), suggesting that the lateralized dendrites present by these ages may be less capable of reorganizing.

The characteristics and dynamic features of the space-filling phenomenon are demonstrated in more detail for two P2 horizontal cells that flanked an ablated cell (Fig. 5a,b). The three cells occupied distinct columnar spaces before ablation. By nine hours post-ablation, exuberant upward and lateral growth into the ablated zone by the two remaining cells left no indication of the initial presence of the targeted cell. The two cells made contact with one another at the approximate midpoint of the ablated zone but did not extend neurites far beyond these appositions. Additionally, growth into the ablated zone did not preclude simultaneous extension in other directions (Fig. 5b).

To quantify the response to larger ablations (7–8 cells ablated), time-lapse images of three fields of P1 horizontal cells were analyzed quantitatively. Territory size increased from 314 ± 20 μm^2 pre-ablation to 418 ± 19 μm^2, seven to eight hours after ablation (Fig. 5d; n = 32; P = 0.001). A slight, further increase was observed eleven to twelve hours post-ablation (459 ± 27 μm^2, P = 0.048). Territory overlap was evaluated at the same intervals. The outermost perimeter of the ablated cells' territories was super-imposed upon the territories of the unablated cells so that neurite extension into the ablated zone could be measured (Fig. 5c). Prior to ablation, the territories of the border cells exhibited 5.2 ± 2.4% overlap with the ablated region (n = 31 border cells; Fig. 5d). This value increased to 26.2 ± 3.7% by eleven to twelve hours post-ablation (Fig. 5d; pre vs. 11–12 hours, $P < 0.001$, Wilcoxon signed rank test). Since overlap with the ablation zone was calculated relative to a fixed perimeter, we also obtained the overlap of each border cell (Fig. 5c) with the initial territory (blue outline) of all border cells at both post-ablation time points (Fig. 5d). Despite the dynamic changes that horizontal cells territories normally exhibit over time (Fig. 4), there was no significant alteration in overlap represented by the blue regions after the ablation (pre vs. 11–12 hours: P = 0.16). Thus, the border cells preferentially elaborated neurites into the ablation zone. Further analysis of post-ablation overlap between the territories of neighboring border cells revealed a small increase in their overlap that was likely secondary to neurite extension into the ablation zone (Fig. 5d; pre vs. 11–12 hours: $P < 0.001$). Together, these data show that (i) the transient vertical neurites of immature horizontal cells possess a growth capacity that is normally constrained by their neighbors, and (ii) such constraints likely arise from repulsive homotypic interactions between the vertical neurites of neighboring cells.

Finally, to assess whether the somata of the border cells moved laterally into the ablation zone, vectors representing the direction and magnitude of post-ablation movement of the soma and center of mass of the territory for each border cell were generated (Fig. 5e). We found that the territories shifted considerably more than somata towards the center of the ablated region (Fig. 5f). In each field (Fig. 5f), we observed a single cell body moving towards the ablation zone (Supplementary Fig. 7 online). Thus, within the time course of imaging (up to 16 hours), the territories of P0–3 horizontal cells oriented towards the ablation regions but cell bodies did not fill these regions.

Interactions may occur between embryonic cells

Although there is no clear exclusion zone in the DRP of embryonic horizontal cells, it remained possible that neurites interact locally. We thus performed ablation experiments in embryonic retina (E17–18). As the distribution of horizontal cells is still relatively sparse and cells occupy different depths at these ages, we ablated only one or two cells that were clearly surrounded by several cells. In one such field, a process extended laterally from a neighboring cell's soma into the space vacated by an ablated cell (Fig. 6a,b). This process maintained its lateral extent and also exhibited vertical growth, creating a clear morphological contrast to the confined columnar architecture of more distant surrounding cells. In a second ablation field, neurites from 4–5 neighbors extended towards the space left by an ablated cell (Fig. 6c,d). These observations suggest that horizontal cells may already exhibit homotypic interactions prior to birth, which are more clearly evident when neighboring cells are removed. Quantification of the movement of the center of mass of the territories (x-y representation) and the somata of cells adjacent to the ablated cell are provided for three ablation fields (Fig. 6e).

Transient vertical neurites do not have synapses

Although the vertical neurites of developing horizontal cells may function to set up the initial territories of horizontal cells, they could also serve as a transient substrate for contact with photoreceptors prior to the elaboration of lateralized dendrites. Horizontal cells and cones are the first differentiated neurons to populate the outer retina and contribute processes to the nascent outer plexiform layer (OPL)7,20,21. Thus, as horizontal cells are undergoing their early postnatal morphological transformation, cone terminals are beginning to target the future OPL. Physical contact between these two cell types has been documented at P322, prior to the appearance of a laminated horizontal cell dendritic arbor. We therefore determined the frequency of these appositions and their spatial distribution relative to the transient vertical neurites of horizontal cells.

Cryosections from P3 and P5 G42 retinas were immunolabeled with VGLUT1 to label cone terminals23 and recoverin to label overall cone morphology24. These ages bracket the restriction of cone terminals and horizontal cell processes to the OPL. Close physical appositions between cone terminals and horizontal cell neurites were numerous in P3 retinas (Fig. 7a,b). Interestingly, these appositions were not found throughout the full depth of the outer retina. Representative images from P3 and P5 (Fig. 7c) demonstrate that even at P3, contacts were restricted to a zone above the horizontal cell somata. The distributions of these contacts were quantified by plotting contacts relative to the average depth of the horizontal

cell somata (Fig. 7d,e), which was used as approximation of the future synaptic lamina. At P3, contacts were found at a mean distance of 10.1 ± 0.4 μm (n = 197 contacts, 3 retinas) from this surface and not more than 25 μm beyond it. By P5, this distribution narrowed to a maximum distance of 10 μm and a significantly lower mean distance of 3.7 ± 0.2 μm by P5 (n = 93 contacts, 2 retinas; $P < 0.001$, Wilcoxon rank sum test). Cone terminals were not found apposed to the prominent vertical neurites of the horizontal cells (Fig. 7c). The transient vertical neurites thus do not appear to function as a substrate for pre-lamination contacts with cones.

DISCUSSION

Migratory paths that position horizontal cells

Mouse horizontal cells in the current study are similar in their radial migratory behavior to horizontal cells in zebrafish25 and chick16 as well as retinal amacrine cells26 and cortical interneurons27. These interneurons all demonstrate migration in the absence of neuritic contact with apical and basal surfaces7,27. Our observations of horizontal cell migration towards the outer retina even after the removal of the pigmented epithelium also suggests that these neurons can attain their correct laminar position independent of extraretinal factors.

Lateral somal translocation along a primary neurite perpendicular to the vertical neurites was unexpected. Our observations of a dilated neurite emanating from the horizontal cell body, followed by the movement of the cell body along this short, laterally-oriented neurite, are consistent with previous descriptions of nucleokinesis in cortical neurons28–30. Furthermore, earlier electron microscopy (EM) data supports the occurrence of nucleokinesis in immature horizontal cells. In morphologically simple cells, such as those we saw migrating radially, EM observations indicate that the centrioles and Golgi apparatus are apical to the nuclei. In contrast, these organelles are lateral to the nuclei of more morphologically complex embryonic horizontal cells in the outer retina7; these cells are shown by the current time-lapse study to undergo lateral somal translocation.

The short distance lateral movement observed in our time-lapse imaging suggests that nucleokinesis may refine somatic position. In fact, these somal movements are consistent with the tangential dispersion of horizontal cells during early retinal development17,18. Our observations of lateral movement at embryonic ages suggest that this behavior begins at birth, which is earlier than previously suggested6. Together, our data indicate that horizontal cells attain their final position by employing both radial migration and lateral somal translocation.

Tiling of radial arbors generate early territories

Computational modeling suggests that lateral cell body movement resulting from homotypic repulsion is sufficient to generate mosaic regularity31. Although such homotypic interactions fail to explain the mosaic organizations of some retinal ganglion cells and amacrine cells32,33, they remain a possible regulatory influence for other retinal neurons and horizontal cells in particular. The regularity of the horizontal cell mosaic is not affected

by photoreceptor loss or the resulting decrease in synapse density10. Local interactions are also implied by the inverse relationship between horizontal cell density and dendritic field size15. Dendritic field size is also at least partially afferent-independent: In the rod-only transgenic mouse, field size is unchanged34. Increased dendritic field size in the cone-only transgenic mouse, however, does indicate that horizontal cell dendritic organization is not solely governed by local homotypic interactions34. Finally, although postnatal apoptosis improves the regularity of some retinal mosaics35, evidence for such cell death in horizontal cells is lacking.

A conundrum, however, is how the lateral dendrites of a horizontal cell can overlap extensively with the dendritic arbors of six to seven neighbors15 and yet generate the homotypic repulsion necessary for the non-random spatial organization of their somata. Although the horizontal cell mosaic collapses following the perturbation of the microtubule-based dendritic scaffold36, there is no direct evidence to implicate dendrites in the initial establishment of the cell somata organization during development. In fact, horizontal cells are non-randomly distributed soon after birth6,37 and before the development of laminar dendritic arbors. Some of this initial regularity could be explained by mechanisms related to cell differentiation38,39, but the mosaic pattern continues to sharpen even before horizontal cells attain a uniform retinal depth37. This refinement suggests that mechanisms acting to position horizontal cells relative to each other are present before the extension of lateral dendrites at P5.

We thus undertook the present study to address whether the transient vertical neurites of immature horizontal cells regulate the early spatial organization of this population. Using the G42 transgenic line and a cell ablation technique, we discovered that vertical neurites form columnar territories that maintain minimal overlap due to homotypic interactions. Interestingly, although cells responded to the ablation of their neighbors by extending vertical neurites into the vacated space, we did not observe a similar colonization of this space by their somata. The absence of somatic movement may be due to the ages (P0–3) at which we performed ablations: The extensive vertical arborization of the neurites may have precluded rapid lateral movements of somata orthogonal to the radial arbor. Future studies that permit similar *in vivo* ablations of horizontal cells are necessary to ascertain whether given sufficient time, cell bodies can move laterally to space-fill. Embryonic ablations also revealed the presence of neuritic interactions between horizontal cells, but at these stages, cells are not yet at similar depths and the nascent mosaic is too sparse to allow substantial analysis of how cell ablation affects regularity. However, it is important to realize that territorial coverage of space is likely to be more important than the exact positioning of cell bodies. We suggest that the neuritic tiling in the early neonates establishes an organized spatial arrangement from which dendrites can later elaborate without being constrained by homotypic repulsion. Together with mechanisms that regulate dendritic growth, such transient tiling could impose some constraint on the future territories and overlap of neighboring horizontal cells. Whether other mechanisms exist to initially position cell bodies during their migration to their lamina remains to be determined.

Could factors other than repulsive homotypic interactions underlie the tiling of the vertical neuritic arbors of the immature horizontal cells? Although tiling and post-ablation neuritic

space-filling could also be explained by competition for a limited shared resource, two observations favor the interpretation that repulsive homotypic interactions between horizontal cells are the underlying mechanism: First, close appositions between the vertical neurites of adjacent cells are present, and second, local changes to the territory are coordinated between neighboring cells to maintain a fixed amount of overlap. Despite the presence of these close appositions, it remains to be determined whether contact-mediated cues alone set the territories of the cells.

Previous ablation studies in retina40,41 showed that altering the local density of the ganglion cell population resulted in a compensatory change in dendritic territory size of nearby ganglion cells. However, because ganglion cells comprise many subtypes, it is unknown whether this response was due to the loss of interactions between cells of the same subtype. In the present study, only homologous cells were ablated, supporting the possibility that the loss of homotypic interactions resulted in the growth of neurites into the ablation zone. This response to ablation is also evident for sensory neurons of the same type in leech1 , *Drosophila*2,3 and larval zebrafish42 for which homotypic repulsive interactions are known to influence tiling of dendritic and axonal arbors. In the retina, ablation of more mature horizontal cells with lateralized dendritic arbors (e.g., P7) did not evoke a rapid in-growth of the dendrites of neighboring cells to space-fill the vacated area. This observation suggests that homotypic interactions between horizontal cells are either absent or much less effective after their vertical neurites disappear. Alternatively, if homotypic dendro-dendritic interactions are present, the lateralized dendrites, when compared to the transient vertical processes, may not have the plasticity to exhibit rapid elaboration when their neighbors are ablated.

Tiling by immature horizontal cells differs in two key respects from other types of neurons. First, and perhaps most obviously, the tiling organization of horizontal cells is established by developmentally transient neurites rather than processes retained through maturity. Second, descriptions of tiling have previously been limited to neurons that possess a planar arbor beginning at their earliest developmental stages. In these systems, outgrowth of dendritic processes ceases when a defined amount of overlap with homotypic neighbors is achieved1,2. Thus, to our knowledge, the present data are the first description of tiling by neurons with arbors that are not yet confined to a single lamina or plane.

It is not currently possible to assess whether the transient neurites are axons, dendrites, or neither. We think they are unlikely to be axons as we can identify axon-like processes at ages when the vertical neurites are present. Further, as appositions with cone terminals do not localize to these neurites, they appear to be distinct from dendrites. Regardless of their identity, it is clear that the transient vertical neurites and the arbors they form have a function distinct from aiding radial cell migration during development of the horizontal cell population.

METHODS

Tissue preparation

All procedures were performed in accordance with Washington University and University of Washington Institutional Animal Care and Use Committee protocols. The day a vaginal plug was detected was defined as embryonic day (E) 1, and birth was defined as postnatal day (P) 0. Animals were anesthetized with 5% halothane or isoflurane and decapitated. Eyes were removed and placed in chilled oxygenated mouse artificial cerebral spinal fluid (mACSF)43, and retinas were removed.

Individual horizontal cells were filled with Alexa Fluor 555 (Invitrogen) using previously described methods44. For immunostaining, retinas were fixed in 4% paraformaldehyde for 20–30 minutes and then washed and stored in 0.1 M phosphate-buffered saline. Retinal whole-mounts were flattened onto black filter paper (Millipore) prior to fixation. Cryostat sections were 20 to 30 μm thick. Immunolabeling was performed using antibodies to detect calbindin (1:1000, Swant; 1:1000, Oncogene Research Products; 1:1000, Calbiochem), recoverin (1:1000, Chemicon), VGLUT1 (1:1000, Chemicon), and GFP (1:1000, Molecular Probes or 1:1000, Chemicon). Antibody amplification was often not necessary for detailed visualization of GFP-expressing neurons in fixed tissue; thus, not all fixed tissue was immunolabeled for GFP. Secondary antibodies were Alexa Fluor 488, 568 or 633 conjugates (1:1000, Molecular Probes). Cytoskeleton labeling of fixed tissue was achieved with Alexa Fluor 633 phalloidin (1:50, Molecular Probes).

Imaging

Fixed tissue was imaged on Olympus FV confocal laser scanning microscopes with Olympus 60x objectives (1.4 and 1.42 NA) and a Zeiss 25x objective (0.8 NA). Live imaging was performed at 890 nm using a Ti:sapphire laser (Spectra-Physics) and a custom-built multiphoton microscope. The z-step (0.5 to 1.0 μm) was determined by the numerical aperture of the 60 x (1.1 NA) objective and the zoom. Each optical plane was averaged three or four times (Kalman filter).

For live imaging, neonatal retinas were either flat-mounted on filter paper or suspended in 1% low melting point agarose that was allowed to set onto the filter paper. Neonatal tissue was superfused with oxygenated mACSF during imaging. For most experiments with embryonic retinas, the tissue was superfused with a carbogen-bubbled culture media45 from which progesterone was omitted. The recording chamber was held at 30–32 °C for imaging of neonatal tissue and 32–34 °C for imaging of embryonic retina. To determine the consequences of cell ablation for the local retinal environment, retinas were incubated in the vital dye BODIPY TR (1:50, Molecular Probes) for two hours before the start of imaging to label cell membranes.

Ablation experiments were conducted with the two-photon microscope. Ablation was performed at 740 nm to avoid GFP photobleaching that could have precluded the visual detection of cell death. Cells within a field were ablated sequentially. A square scanning area with sides of 3 μm was centered on the brightest plane of the target cell body. Laser

power (600–900 mW at the scanhead) and the ablation parameters were optimized for each experiment.

Analysis and statistics

Image processing—Images were processed using MetaMorph (Universal Imaging) and Amira (Mercury Computer Systems). When analysis of individual horizontal cells was necessary, cells were segmented plane-by-plane and colorized. A median or Gaussian filter was applied to segmented cells to reduce detector noise.

Territories, overlap and contact—Horizontal cells were assigned a two-dimensional territory with a custom Matlab program (MathWorks) based on erosion-dilation functions46. Since GFP expression by horizontal cells at a population level is incomplete in the G42 retina, overlap was considered on a pair-wise basis. Cell pairs that demonstrated overlap of their territories at any time point of the recording were included in the data set for the plots shown in Figure 4.

Measurements of contact depth between cone terminals and horizontal cell processes were made in Metamorph. Points of contact were identified by scrolling through the combined GFP and VGLUT1 image stacks, plane-by-plane, and the z-stacks were rotated if the status of a potential apposition remained ambiguous.

Center of mass of territories and cell movement after ablation—The center of mass of the two-dimensional territories of each cell adjacent to the ablation region was obtained using a MatLab routine. The distance of the center of the soma and the center of mass of the territory from the center of mass of the ablation area was obtained for each border cell before and after ablation to generate the vector diagram (Fig. 5e).

Density recovery profile—In this study, the autocorrelation plots display the 2D spatial relationship of each pair of cells within 50 μm of each other (and more than 50 μm from the image border). The density recovery profile (DRP) is a plot of the density of horizontal cells as a function of a radial distance from each horizontal cell within the field19. A dip in the DRP near the point of reference (0,0; center of the cell body) below the average density demonstrates that there is a spatial region surrounding the cell within which there is a decreased probability of finding another cell. We normalized the somal density to the mean density of the cells found within the field. For a given mean density, the flat line at a density of 1.0 of the DRP represents the expected distribution for the horizontal cells if the distribution of the center of the somata (a point) was random (Poisson). The effective radius is a quantitative measure derived from the DRP that indicates the size of the region of decreased cell density. This measure is insensitive to under-sampling of the distribution. The DRPs were obtained by using a routine written in MatLab.

Statistics—Statistical analysis for paired observations was performed using the Wilcoxon signed rank test in Matlab. Analysis of unpaired observations was performed using the Mann-Whitney test in Matlab.

Supplementary Material

Refer to Web version on PubMed Central for supplementary material.

ACKNOWLEDGEMENTS

Supported by NIH grants to R.O. Wong (EY17101) and J.Z. Huang, and an NRSA (NIH) pre-doctoral fellowship to R.M.H. We wish to thank Dr. Stephen Eglen (Cambridge University) and members of the Wong lab for many helpful discussions.

REFERENCES

1. Gan WB, Macagno ER. Interactions between segmental homologs and between isoneuronal branches guide the formation of sensory terminal fields. J Neurosci. 1995; 15:3243–3253. [PubMed: 7751907]
2. Grueber WB, Ye B, Moore AW, Jan LY, Jan YN. Dendrites of distinct classes of Drosophila sensory neurons show different capacities for homotypic repulsion. Curr Biol. 2003; 13:618–626. [PubMed: 12699617]
3. Sugimura K, et al. Distinct developmental modes and lesion-induced reactions of dendrites of two classes of Drosophila sensory neurons. J Neurosci. 2003; 23:3752–3760. [PubMed: 12736346]
4. Wassle H, Peichl L, Boycott BB. Mosaics and territories of cat retinal ganglion cells. Prog Brain Res. 1983; 58:183–190. [PubMed: 6195688]
5. Vaney DI. The mosaic of amacrine cells in the mammalian retina. Progress in Retinal Research. 1990; 9:49–100.
6. Raven MA, Stagg SB, Nassar H, Reese BE. Developmental improvement in the regularity and packing of mouse horizontal cells: implications for mechanisms underlying mosaic pattern formation. Vis Neurosci. 2005; 22:569–573. [PubMed: 16332267]
7. Hinds JW, Hinds PL. Differentiation of photoreceptors and horizontal cells in the embryonic mouse retina: an electron microscopic, serial section analysis. J Comp Neurol. 1979; 187:495–511. [PubMed: 489789]
8. Schnitzer J, Rusoff AC. Horizontal cells of the mouse retina contain glutamic acid decarboxylase-like immunoreactivity during early developmental stages. J Neurosci. 1984; 4:2948–2955. [PubMed: 6502214]
9. Poche RA, et al. Somal positioning and dendritic growth of horizontal cells are regulated by interactions with homotypic neighbors. Eur J Neurosci. 2008; 27:1607–1614. [PubMed: 18380663]
10. Rossi C, Strettoi E, Galli-Resta L. The spatial order of horizontal cells is not affected by massive alterations in the organization of other retinal cells. J Neurosci. 2003; 23:9924–9928. [PubMed: 14586022]
11. Chattopadhyaya B, et al. Experience and activity-dependent maturation of perisomatic GABAergic innervation in primary visual cortex during a postnatal critical period. J Neurosci. 2004; 24:9598–9611. [PubMed: 15509747]
12. Peichl L, Gonzalez-Soriano J. Morphological types of horizontal cell in rodent retinae: a comparison of rat, mouse, gerbil, and guinea pig. Vis Neurosci. 1994; 11:501–517. [PubMed: 8038125]
13. Haverkamp S, Wassle H. Immunocytochemical analysis of the mouse retina. J Comp Neurol. 2000; 424:1–23. [PubMed: 10888735]
14. Ramón y Cajal, S. Studies on vertebrate neurogenesis. Springfield, Ill.: Thomas; 1960.
15. Reese BE, Raven MA, Stagg SB. Afferents and homotypic neighbors regulate horizontal cell morphology, connectivity, and retinal coverage. J Neurosci. 2005; 25:2167–2175. [PubMed: 15745942]
16. Edqvist PH, Hallbook F. Newborn horizontal cells migrate bi-directionally across the neuroepithelium during retinal development. Development. 2004; 131:1343–1351. [PubMed: 14973293]

17. Reese BE, Harvey AR, Tan SS. Radial and tangential dispersion patterns in the mouse retina are cell-class specific. Proc Natl Acad Sci U S A. 1995; 92:2494–2498. [PubMed: 7708672]
18. Reese BE, Necessary BD, Tam PP, Faulkner-Jones B, Tan SS. Clonal expansion and cell dispersion in the developing mouse retina. Eur J Neurosci. 1999; 11:2965–2978. [PubMed: 10457191]
19. Rodieck RW. The density recovery profile: a method for the analysis of points in the plane applicable to retinal studies. Vis Neurosci. 1991; 6:95–111. [PubMed: 2049333]
20. Blanks JC, Adinolfi AM, Lolley RN. Synaptogenesis in the photoreceptor terminal of the mouse retina. J Comp Neurol. 1974; 156:81–93. [PubMed: 4836656]
21. Young RW. Cell proliferation during postnatal development of the retina in the mouse. Brain Res. 1985; 353:229–239. [PubMed: 4041905]
22. Rich KA, Zhan Y, Blanks JC. Migration and synaptogenesis of cone photoreceptors in the developing mouse retina. J Comp Neurol. 1997; 388:47–63. [PubMed: 9364238]
23. Sherry DM, Wang MM, Bates J, Frishman LJ. Expression of vesicular glutamate transporter 1 in the mouse retina reveals temporal ordering in development of rod vs. cone and ON vs. OFF circuits. J Comp Neurol. 2003; 465:480–498. [PubMed: 12975811]
24. Sharma RK, O'Leary TE, Fields CM, Johnson DA. Development of the outer retina in the mouse. Brain Res Dev Brain Res. 2003; 145:93–105. [PubMed: 14519497]
25. Godinho L, et al. Nonapical symmetric divisions underlie horizontal cell layer formation in the developing retina in vivo. Neuron. 2007; 56:597–603. [PubMed: 18031679]
26. Godinho L, et al. Targeting of amacrine cell neurites to appropriate synaptic laminae in the developing zebrafish retina. Development. 2005; 132:5069–5079. [PubMed: 16258076]
27. Nadarajah B, Alifragis P, Wong RO, Parnavelas JG. Neuronal migration in the developing cerebral cortex: observations based on real-time imaging. Cereb Cortex. 2003; 13:607–611. [PubMed: 12764035]
28. Solecki DJ, Model L, Gaetz J, Kapoor TM, Hatten ME. Par6alpha signaling controls glial-guided neuronal migration. Nat Neurosci. 2004; 7:1195–1203. [PubMed: 15475953]
29. Bellion A, Baudoin JP, Alvarez C, Bornens M, Metin C. Nucleokinesis in tangentially migrating neurons comprises two alternating phases: forward migration of the Golgi/centrosome associated with centrosome splitting and myosin contraction at the rear. J Neurosci. 2005; 25:5691–5699. [PubMed: 15958735]
30. Schaar BT, McConnell SK. Cytoskeletal coordination during neuronal migration. Proc Natl Acad Sci U S A. 2005; 102:13652–13657. [PubMed: 16174753]
31. Eglen SJ, van Ooyen A, Willshaw DJ. Lateral cell movement driven by dendritic interactions is sufficient to form retinal mosaics. Network. 2000; 11:103–118. [PubMed: 10735531]
32. Lin B, Wang SW, Masland RH. Retinal ganglion cell type, size, and spacing can be specified independent of homotypic dendritic contacts. Neuron. 2004; 43:475–485. [PubMed: 15312647]
33. Farajian R, Raven MA, Cusato K, Reese BE. Cellular positioning and dendritic field size of cholinergic amacrine cells are impervious to early ablation of neighboring cells in the mouse retina. Vis Neurosci. 2004; 21:13–22. [PubMed: 15137578]
34. Raven MA, Oh EC, Swaroop A, Reese BE. Afferent control of horizontal cell morphology revealed by genetic respecification of rods and cones. J Neurosci. 2007; 27:3540–3547. [PubMed: 17392470]
35. Jeyarasasingam G, Snider CJ, Ratto GM, Chalupa LM. Activity-regulated cell death contributes to the formation of ON and OFF alpha ganglion cell mosaics. J Comp Neurol. 1998; 394:335–343. [PubMed: 9579397]
36. Galli-Resta L, Novelli E, Viegi A. Dynamic microtubule-dependent interactions position homotypic neurones in regular monolayered arrays during retinal development. Development. 2002; 129:3803–3814. [PubMed: 12135919]
37. Novelli E, Leone P, Resta V, Galli-Resta L. A three-dimensional analysis of the development of the horizontal cell mosaic in the rat retina: implications for the mechanisms controlling pattern formation. Vis Neurosci. 2007; 24:91–98. [PubMed: 17430612]

38. Tyler MJ, Carney LH, Cameron DA. Control of cellular pattern formation in the vertebrate inner retina by homotypic regulation of cell-fate decisions. J Neurosci. 2005; 25:4565–4576. [PubMed: 15872104]

39. McCabe KL, Gunther EC, Reh TA. The development of the pattern of retinal ganglion cells in the chick retina: mechanisms that control differentiation. Development. 1999; 126:5713–5724. [PubMed: 10572047]

40. Perry VH, Linden R. Evidence for dendritic competition in the developing retina. Nature. 1982; 297:683–685. [PubMed: 7088156]

41. Hitchcock PF. Exclusionary dendritic interactions in the retina of the goldfish. Development. 1989; 106:589–598. [PubMed: 2598827]

42. Sagasti A, Guido MR, Raible DW, Schier AF. Repulsive interactions shape the morphologies and functional arrangement of zebrafish peripheral sensory arbors. Curr Biol. 2005; 15:804–814. [PubMed: 15886097]

43. Stacy RC, Wong RO. Developmental relationship between cholinergic amacrine cell processes and ganglion cell dendrites of the mouse retina. J Comp Neurol. 2003; 456:154–166. [PubMed: 12509872]

44. Shelley J, et al. Horizontal cell receptive fields are reduced in connexin57-deficient mice. Eur J Neurosci. 2006; 23:3176–3186. [PubMed: 16820008]

45. Roberts MR, Srinivas M, Forrest D, Morreale de Escobar G, Reh TA. Making the gradient: thyroid hormone regulates cone opsin expression in the developing mouse retina. Proc Natl Acad Sci U S A. 2006; 103:6218–6223. [PubMed: 16606843]

46. Morgan JL, Schubert T, Wong RO. Developmental patterning of glutamatergic synapses onto retinal ganglion cells. Neural Develop. 2008; 3:8.

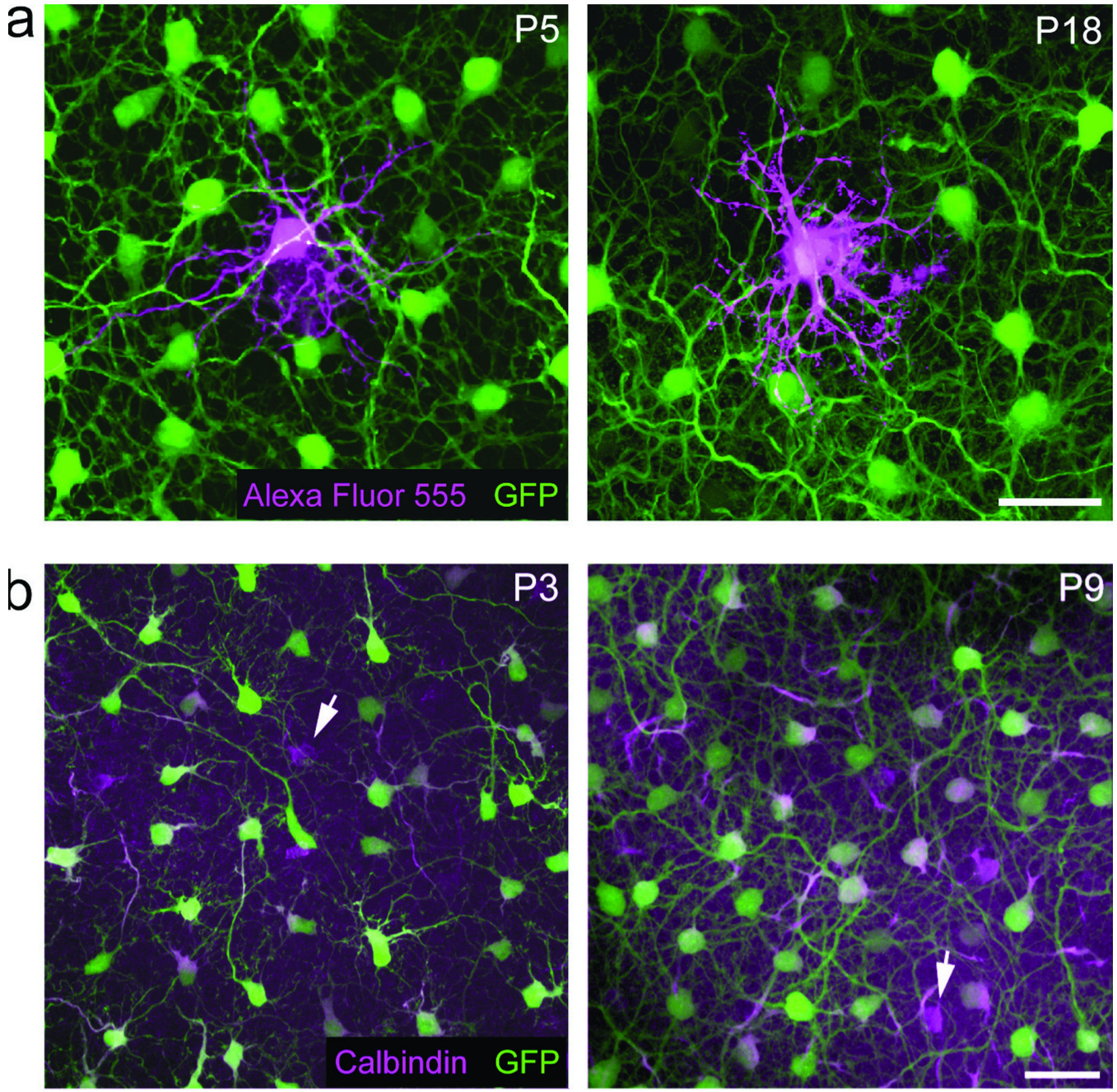

Figure 1. Horizontal cells in the G42 retina express GFP

(**a**) Intracellular dye-filling of a GFP-positive horizontal cell in a P5 and P18 G42 retina. (**b**) Immunostaining for calbindin at P3 and P9 demonstrates that most of the horizontal cell population is represented in regions of dense GFP expression. Arrows indicate examples of occasional calbindin-positive cells that were GFP-negative. Scale bar, 30 μm.

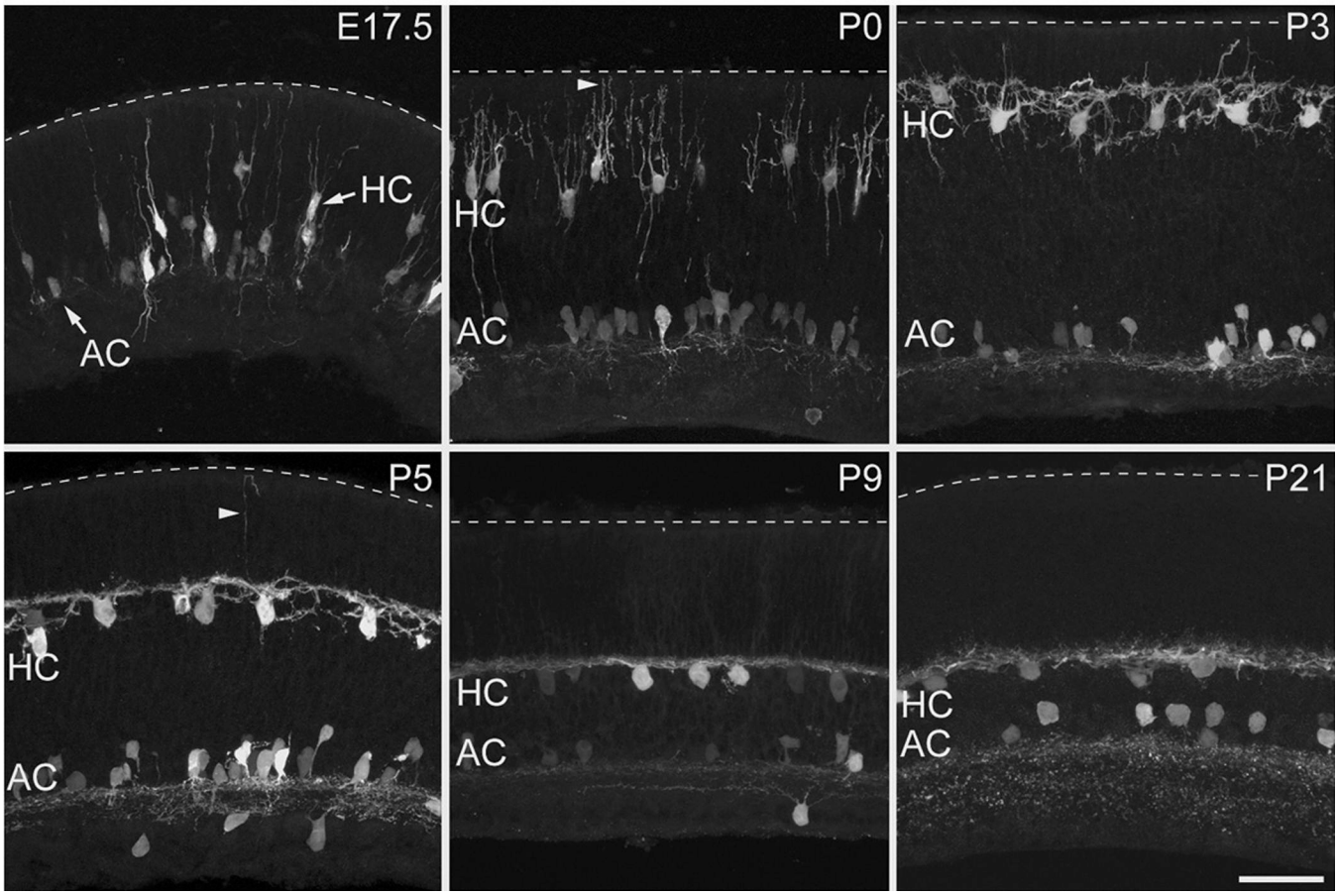

Figure 2. Positioning of horizontal cells within the correct lamina is accompanied by reorganization of their neurites

Cross-sections from embryonic and neonatal G42 retinas demonstrate the migration and changes in morphology of horizontal cells (HC) with age. Transient vertical neurites (arrowheads) of horizontal cells are replaced by lateralized dendrites with maturation. Dotted line indicates the outer limiting membrane (OLM). AC, amacrine cells. Scale bar, 40 μm.

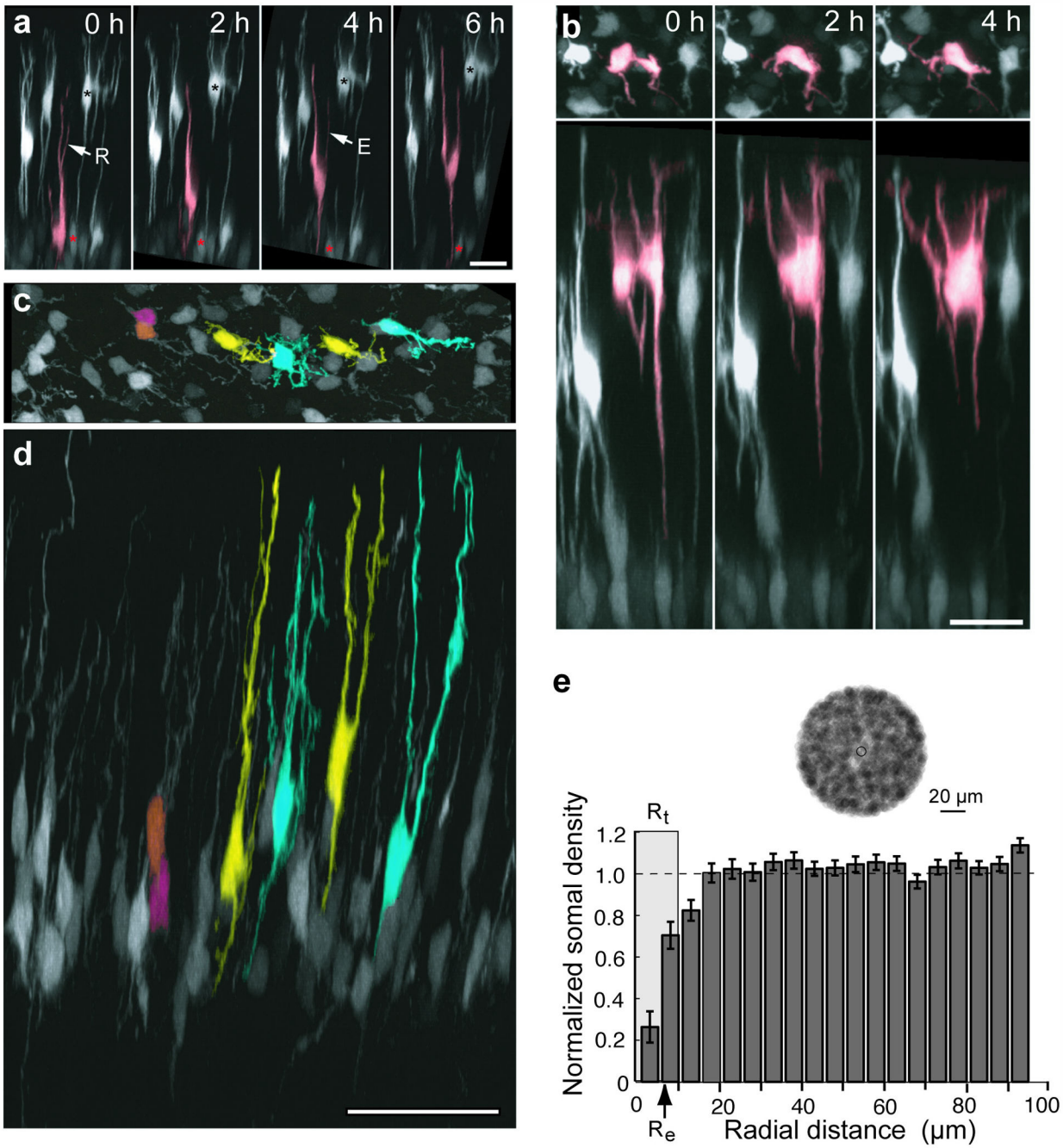

Figure 3. Embryonic horizontal cells exhibit free migration and lateral somal translocation

(**a**) Vertical migration of an E17.5 horizontal cell (red) relative to a horizontal cell at the outer retina (black asterisk) and an amacrine cell (red asterisk). Examples of extension (E) and retraction (R) of vertical neurites. Scale bar, 20 µm.

(**b**) Lateral translocation of an E17.5 horizontal cell soma in the outer retina as seen *en face* (top panels) and in orthogonal views (bottom panels). Scale bar, 20 µm.

(**c,d**) *En face* (**c**) and orthogonal (**d**) views of E17 horizontal cells. Yellow and blue cells illustrate the narrow vertical distribution of the neuritic processes. Apparent somal overlap in the *en face* view reflects different cell depths (e.g. orange and red cells). Scale bar, 50 μm. (**e**) Density recovery profile for E17–18 horizontal cells (n = 388 cells). The distribution was normalized to the mean spatial density (dotted line) of the image field. If cell bodies are randomly distributed, the profile is flat. Light grey bar indicates the equivalent radius (R_t) of the neuritic territories and arrow indicates the effective radius (R_e). An example of a spatial auto-correlogram is shown above the DRP; there is no empty zone within 50 μm of the reference point (unshaded circle). Each circle represents a soma of radius 3.6 μm. Error bars = S.E.M.

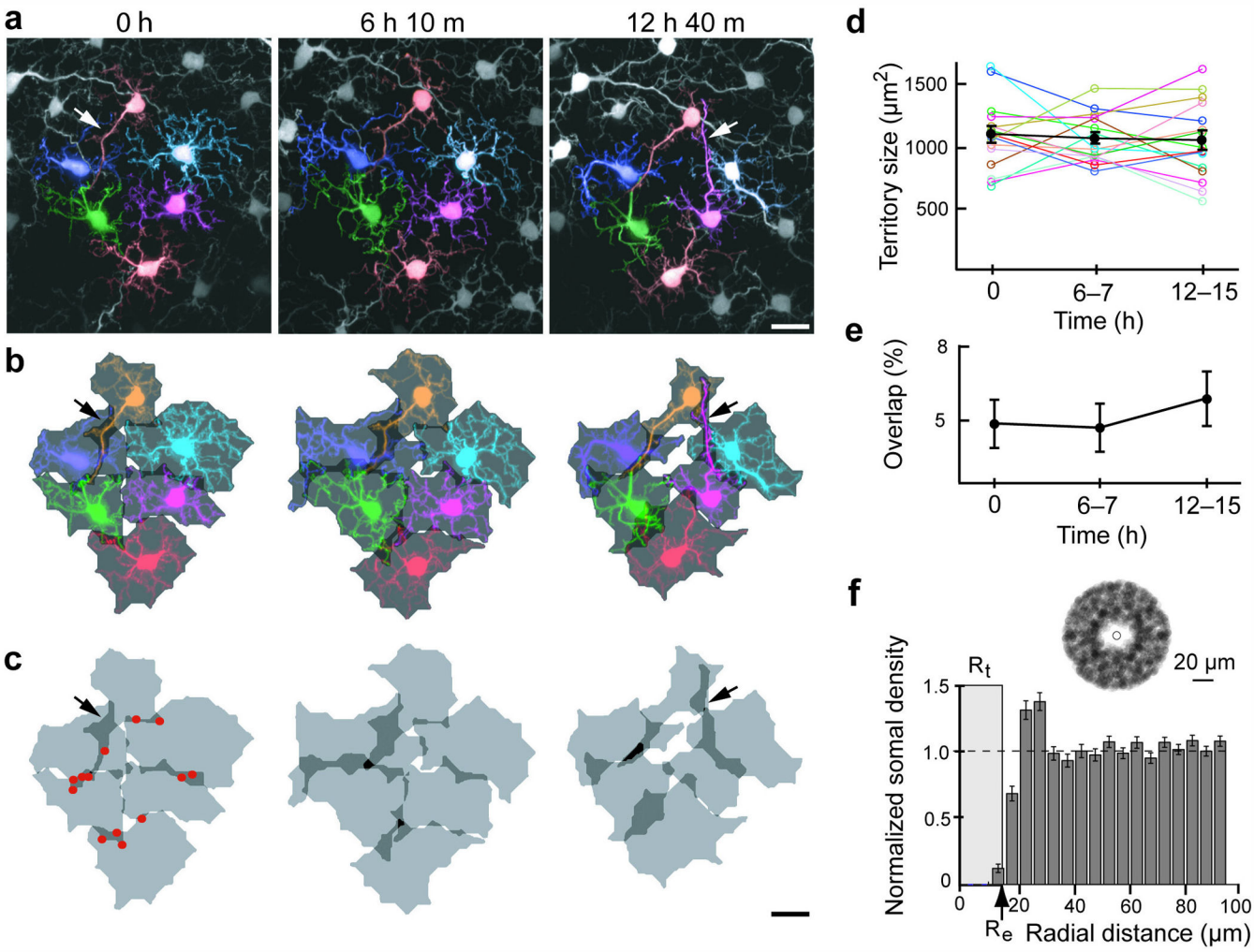

Figure 4. Vertical neurites form territories with minimal and stable overlap

(**a**) A field of P2 horizontal cells was followed over time. Cells were segmented and colorized to allow visualization of the neurites of individual cells.

(**b-c**) Each segmented cell was assigned a two-dimensional territory based on the distribution of its neurites (see Methods). Arrows indicate axon-like processes that were included in the territory assignments. Dark grey areas in (**c**) indicate overlap between two adjacent territories and black areas represent overlap between three territories. Red dots indicate point of apposition.

(**d**) Individual and mean territory sizes over time (16 cells, 3 retinas).

(**e**) Mean overlap between adjacent territories of pairs of neighboring cells over time (16 cells, 3 retinas).

(**f**) Density recovery profile (histogram) of horizontal cells from P2 (n = 265 cells). Light grey bar indicates the equivalent radius (R_t) of horizontal cell territories at these ages and arrow indicates the effective radius (R_e) for the DRP. An example of a spatial auto-correlogram is shown above the DRP; note there is an empty zone within about 20 μm of the central reference point (unshaded circle). Each circle represents a cell body with diameter of 3.8 μm.

All scale bars, 15 μm. Error bars = S.E.M.

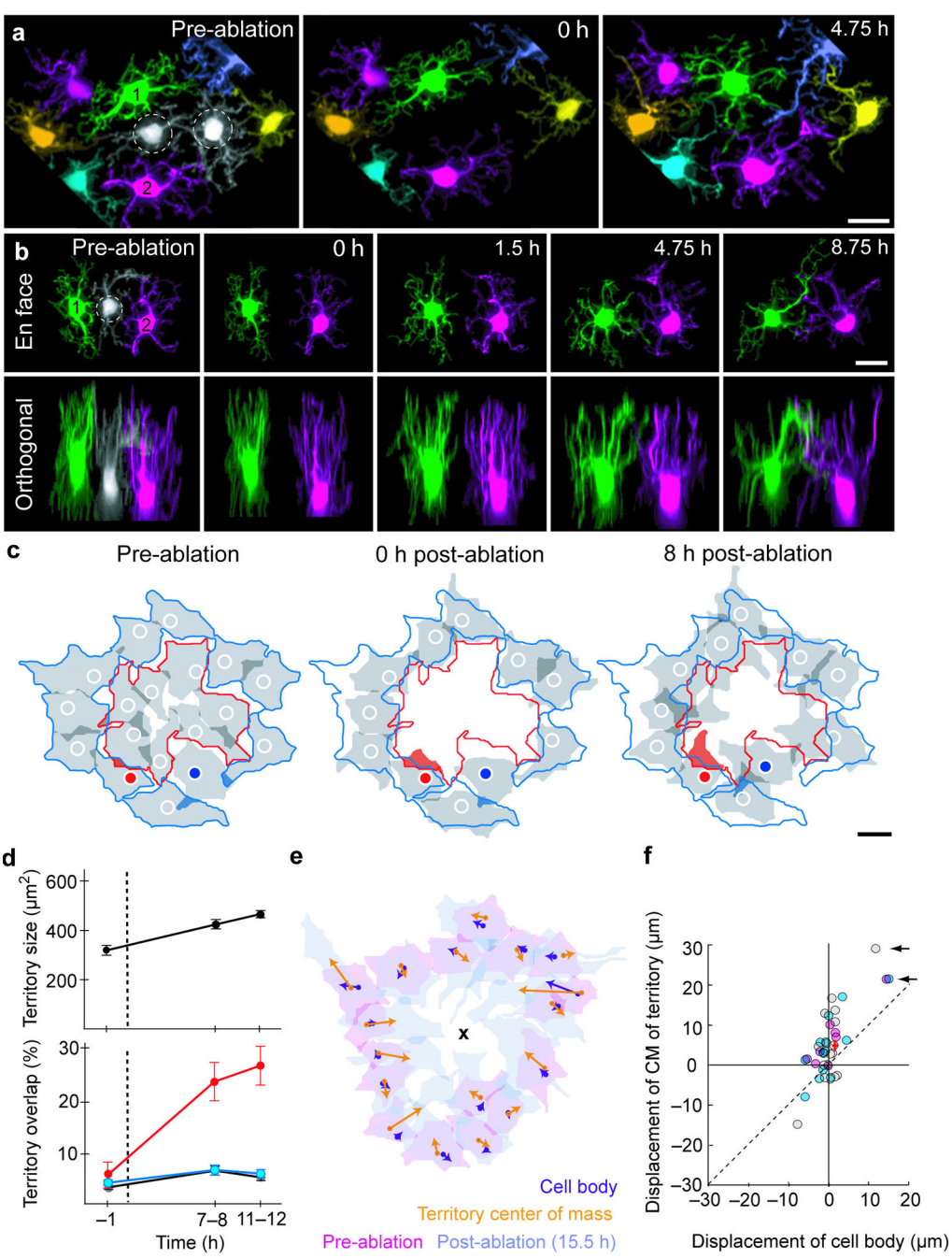

Figure 5. Transient vertical neurites exhibit homotypic interactions

(**a,b**) Ablation of horizontal cells (dotted circles) evoked neurite extension by neighbors (Supplementary Video 2).

(**c**) Territory analysis at P1 after ablation of seven cells. Grey: Individual cell territories. Red outline: Outermost perimeter of the ablated cell territories. White circles: Somata. Red shading: Overlap of border cell (red dot) with ablated zone. Blue shading: Overlap of border cell (blue dot) territory with outline of the combined pre-ablation border cell territories (blue perimeter).

(**d**) Mean territory size and overlap before and after ablation (3 retinas, 31 cells). Dotted line: Time of ablation. Red: Overlap between border cells and ablation zone. Blue: Overlap between border cells and the initial territory occupied by the border cells (38 cells). Black: Overlap of the individual territories of border cell pairs (dark grey areas) at each time point. Territorial overlap represents the % area of a cell's total territory that is shared with a neighbor or which extends into the perimeter of the ablation zone. Error bars = S.E.M.
(**e**) Vector diagram showing post-ablation displacement of cell bodies and territory centers of mass. X = Ablation zone center of mass.
(**f**) Post-ablation displacements of border cell somata and the center of mass (CM) of their territories. Each color represents cells from one recording field. Positive values in the x and y axes indicate displacement towards the ablation region. Arrows indicate cells with relatively large displacements of both cell somata and CM of territory.
All scale bars, 15 μm.

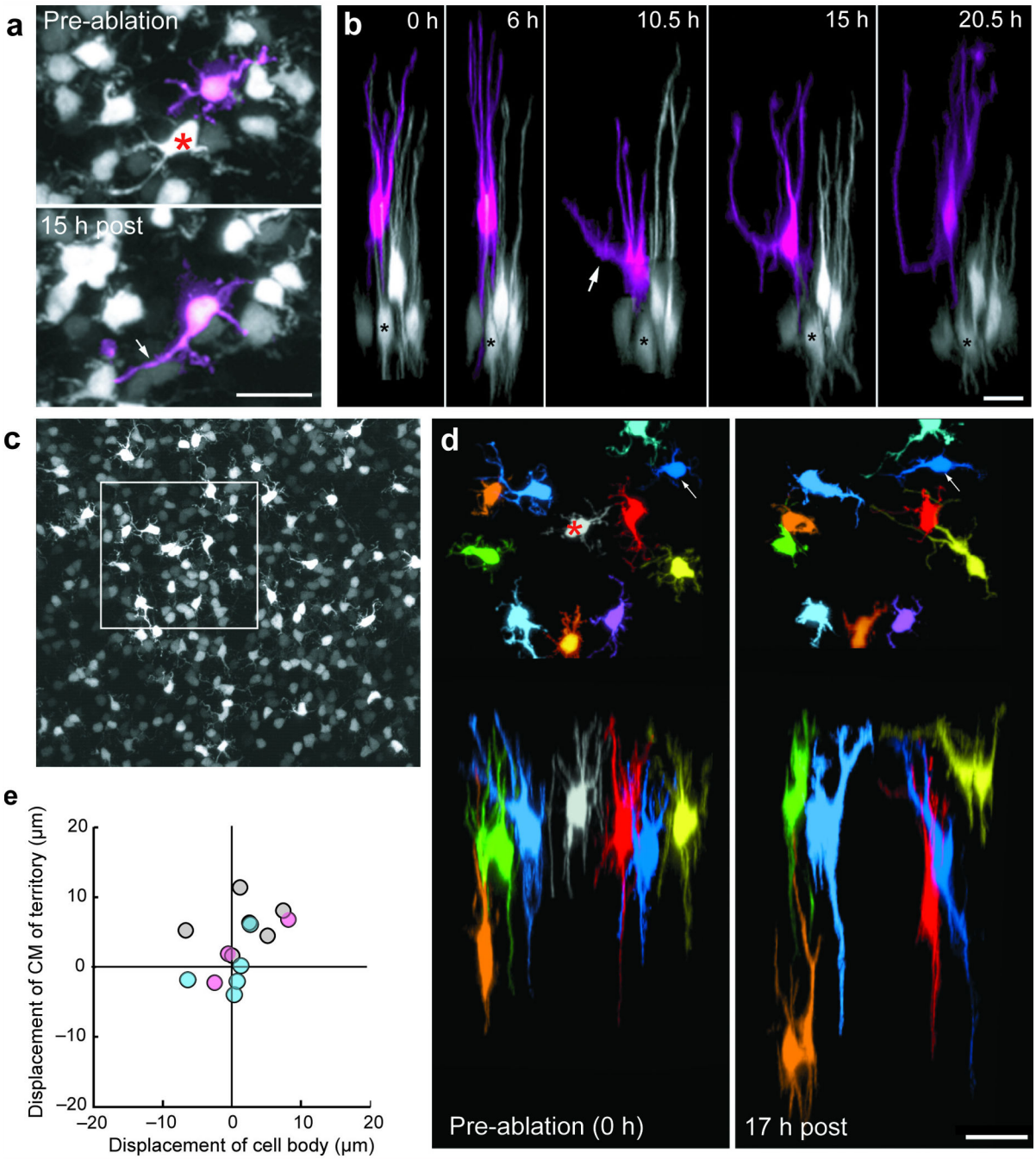

Figure 6. Homotypic interactions are present between embryonic horizontal cells

(**a**) A single horizontal cell (red asterisk) was ablated in an E17.5 retina. In the hours following ablation, an adjacent horizontal cell (magenta) extended neurites laterally (arrow) across the space that was previously occupied by the ablated cell.

(**b**) Orthogonal views of the segmented cell in (**a**). At 6 hours post-ablation, the columnar organization of its vertical neurites and its depth relative to a nearby horizontal cell (asterisk) were unchanged. At 10.5 hours post-ablation, a process extended laterally (arrow)

and the cell moved towards the inner retina. This lateral neurite exhibited vertical growth and the cell body moved upwards to re-establish its initial depth. Scale bar (**a,b**), 15 μm. (**c,d**) A low magnification view of a region of horizontal cells at E17.5. A cell within the boxed region (**c**) was ablated and the neurites of pseudocolored neighboring cells were followed over time (**d**). Arrow indicates a cell that showed significant displacement of the soma towards the location of the ablated cell. More prominent are the extension of neurites of some cells towards the vacated space. Scale bar (**d**), 15 μm.

(**e**) Plot of the center of mass (CM) and somal movements after cell ablation at embryonic ages (n = 3 retinas). Each color represents cells within each image field. Because of the sparse distribution of cells at embryonic ages, only cells adjacent to the ablated cell were included for analysis.

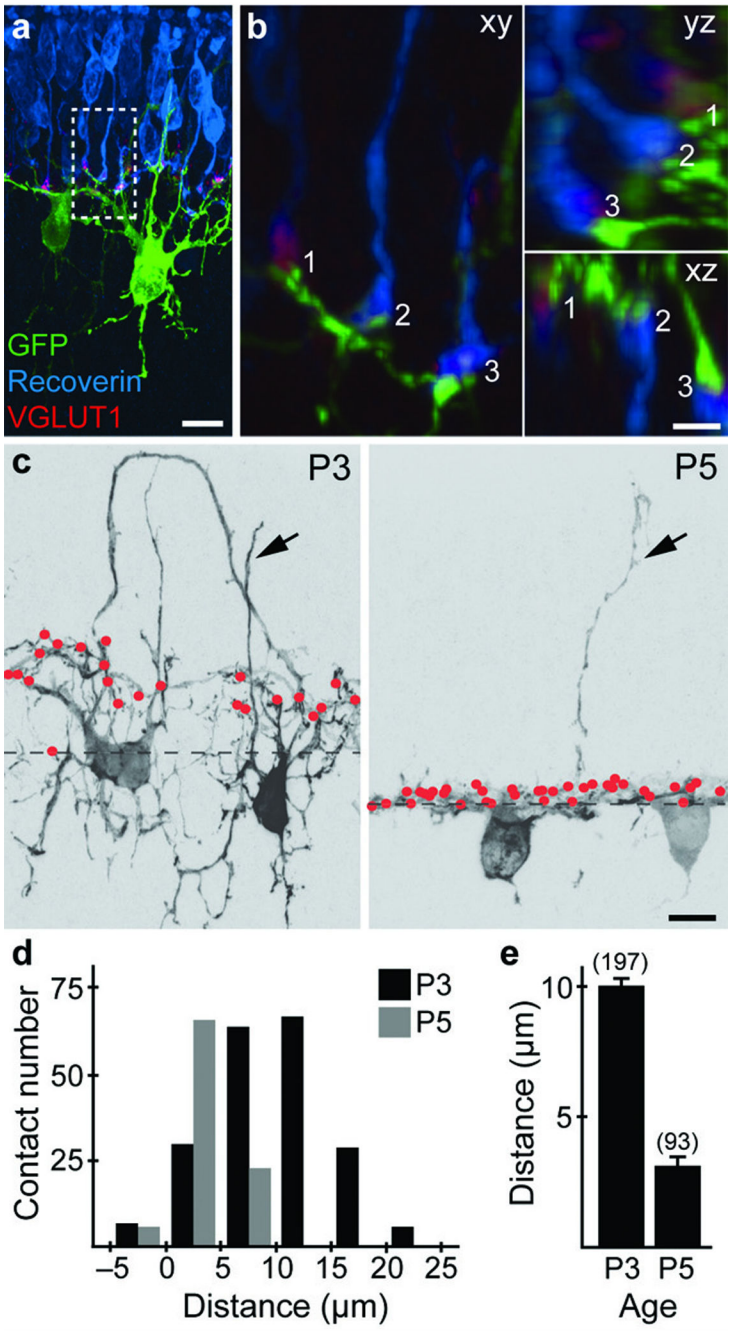

Figure 7. Vertical neurites do not appear to be contacted by cone terminals

(**a**) Immunostaining for cones (recoverin), their terminals (VGLUT1), and horizontal cells (GFP) in a cryosection from a P3 G42 retina.

(**b**) Rotations of image stacks encompassing the region of appositions between horizontal cell processes and cone terminals found within the inset in (**a**).

(**c**) Red dots indicate positions of appositions between cone terminals and horizontal cells in typical P3 and P5 retinas. Appositions did not localize to the vertical neurites (arrows) of

horizontal cells. Dotted line indicates the average depth horizontal cell somata within the field of view.

(**d**) Spatial distributions of appositions at P3 and P5 relative to the average depth of horizontal cell somata (dashed line in **c**).

(**e**) Mean distance of appositions at P3 and P5 relative to the average depth of horizontal cell somata (dashed line in **c**). Error bars = S.E.M.

Scale bars (**a,c**), 15 μm; scale bar (**b**), 5 μm.